*Soc.*, **48**, 133 (1949).
9. W. R. Foster, *J. Am. Ceram. Soc.*, **34**, 302 (1951).
10. C. E. Curtis and H. G. Sowman, *ibid.*, **36**, 190 (1953).
11. G. M. Matwejew and A. S. Agarkow, *Silikat Tech.*, **20**, 86 (1969).
12. J. Elliot, M. Gleiser, and V. Ramarkrishna, "Thermochemistry for Steelmaking," Vol. II. Addison Wesley, New York (1963).
13. JANAF Thermochemical Tables, Second edition, Nat. Stand. Ref. Data Ser., Nat. Bur. Std. (U.S.), 37 (June 1971).
14. H. H. Kellog, *Trans. Met. Soc. AIME*, **236**, 602 (1966).
15. E. A. Gulbransen and S. A. Jansson, Paper presented at the International Conference on Heterogenous Kinetics at Elevated Temperatures, Philadelphia, Sept. 8-10, 1969.
16. N. C. Tombs and A. J. E. Welch, *J. Iron Steel Inst.*, **172**, 69 (1952).
17. H. Schafer and R. Hornle, *Z. Anorg. Allgem. Chem.*, **263**, 261 (1950).
18. G. Grube and H. Speidel, *Z. Electrochem.*, **53**, 339 (1949).
19. H. F. Ramstad and F. D. Richardson with Appendix by P. J. Bowles, *Trans. Met. Soc. AIME*, **221**, 1021 (1961).
20. K. G. Gunther, *Glastech. Ber.*, **31**, 15 (1958).
21. P. V. Gel'd and M. K. Kochnev, *Zh. Prikl. Khim.*, **21**, 1249 (1948).
22. G. L. Humphrey, S. S. Todd, J. P. Coughlin, and E. G. King, *U.S. Bur. Mines Bull.*, 4888 (1952).
23. O. Meyer, *Arch. Eisenhuettenw.*, **4**, 193 (1930).
24. W. Eitel, "Silicate Science," Vol. V, pp. 183-184, Academic Press, New York (1966).
25. E. Steinhoff, *Glastech. Ber.*, **33**, 86 (1960).
26. K. Schwerdtfeger, *Trans. Met. Soc. AIME*, **236**, 1152 (1966).
27. M. S. Crowley, *Bull. Am. Ceram. Soc.*, **46**, 679 (1967).
28. M. S. Crowley, *ibid.*, **49**, 527 (1960).
29. R. A. Gardner, *J. Solid State Chemistry*, **9**, 336 (1974).
30. J. D. Hancock and J. H. Sharp, *J. Am. Ceram. Soc.*, **55**, 74 (1972).
31. R. A. Gardner and W. R. Swiss, *Rev. Sci. Instr.*, **44**, 1428 (1973).

# Electrohydrodimerization Reactions

## IV. A Study of the Effect of Alkali Metal Ions on the Hydrodimerization of Several 1,2-Diactivated Olefins in DMF Solutions by Chronoamperometry and Chronocoulometry

**Mark J. Hazelrigg, Jr. and Allen J. Bard***

*Department of Chemistry, The University of Texas at Austin, Austin, Texas 78712*

ABSTRACT

The reduction of the activated olefins: dialkyl fumarates (alkyl = methyl, ethyl, butyl), ethyl cinnamate and cinnamonitrile in tetra-n-butylammonium iodide-dimethylformamide solutions in the absence and presence of $Li^+$, $Na^+$, and $K^+$ was studied by double potential step chronocoulometric and chronoamperometric techniques, cyclic voltammetry, and controlled potential coulometry. The results in the absence of alkali metal ions confirmed the previous mechanism involving formation of the radical anion, $R^-$, followed by dimerization; no evidence of appreciable adsorption of the parent olefin or $R^-$ was found. The addition of alkali metal ion ($M^+$) greatly increased the rate of the dimerization reaction and a mechanism based on formation of the ion pair, $M^+R^-$, followed by reaction of $M^+R^-$ with $R^-$ or coupling of two $M^+R^-$ species is proposed based on an analysis of the kinetic data. The addition of $Li^+$ also decreased the extent of polymer formation during bulk electrolysis experiments.

The mechanism of electrohydrodimerizations (1) (Eq. [1]) of activated olefins and related substances has been the subject of numerous investigations

$$2R + 2H^+ + 2e \rightarrow R_2H_2 \qquad [1]$$

in recent years. The mechanism which has emerged, based on chronoamperometric (2), rotating ring-disk electrode (3, 4), electron spin resonance (ESR) spectroscopic (5), linear scan voltammetric (6, 7), chronopotentiometric (8), and a-c polarographic (9) studies, is one in which the predominant pathway for many compounds (*e.g.*, dialkyl fumarates, cinnamonitrile, $\alpha,\beta$-unsaturated ketones) is an initial one-electron transfer at an electrode followed by dimerization of the electrogenerated radical ions (Eq. [2] and [3]), followed by protonation

$$R + e \rightarrow R^- \qquad [2]$$

$$2R^- \xrightarrow{k_2} R_2^{2-} \qquad [3]$$

* Electrochemical Society Active Member.

Key words: reductive coupling, electrolytic dimerizations, voltammetry, coulometry, ion pair formation.

Previous studies of electrohydrodimerizations of activated olefins have shown a strong effect on the electrochemical behavior on addition of alkali metal ions. Baizer (1, 10) for example, showed that the product ratios and reaction paths in reductive coupling depend upon the cation of the supporting electrolyte. Previous studies from this laboratory on the reduction of diethyl fumarate in N,N-dimethylformamide (DMF) solutions (2) showed that the addition of $LiClO_4 \cdot 3H_2O$ in millimolar concentrations to DMF solutions containing 0.44M tetra-n-butylammonium iodide (TBAI) caused the controlled potential coulometric $n_{app}$-value (where $n_{app}$ is the number of faradays consumed per mole of electroactive species) to increase from 0.6 to 1.0, indicating an increase in the extent of formation of hydrodimer and a decrease in polymer formation. The addition of these small amounts of $LiClO_4$ also was found to increase the rate of the dimerization of the radical ions, although a quantitative study of this was not undertaken.

The alkali metal ion effect is most probably attributable to ion-pair formation between the alkali metal ion and the olefin radical anion. Ion-pair formation of

radical anions of organic compounds with metal ions in aprotic solvents has been of interest and has been studied using ESR and absorption spectroscopy (11), and polarography (12-15). Most of the previous electrochemical studies have been concerned with anions of aromatic quinones, nitrocompounds or carbonyl compounds. Very little work has been done with ion-pairs involving olefin anions. Ion-pairing affects the electrochemical reduction of organic compounds in different ways depending upon the electrochemical and chemical reactivity of the ion-pair. For the Nernstian reduction of neutral compounds which form stable radical anions, ion-pair formation causes a positive shift in $E_{1/2}$ or $E_{pc}$; this shift in the reduction potential can be used to determine the ion-pair formation constant, $K$, (Eq. [4]) where $\Delta E$ is

$$\Delta E = (RT/n\mathbf{F})\ln(1 + K[M^+]) \qquad [4]$$

the shift in reduction potential, $[M^+]$ is the metal ion concentration, and $K$ is the ion-pair formation constant. For example, Peover and Davis (12) found an ion-pair formation constant for the $Li^+$-anthrasemiquinone ion-pair in 0.1M TEAP-DMF of 39 liters/mole using this method.

Ion-pair formation has also been shown to affect the rate of reactions following the electron transfer step. For example, Philp, Layloff, and Adams (16) found that $Li^+$ changes the electrochemical reduction pathway of benzil. In the absence of $Li^+$, benzil is reduced in DMF solutions in 2 one-electron steps, while in the presence of $Li^+$, it is reduced in an over-all single two-electron step. They proposed that a $Li^+$-benzil$^-$ ion-pair is formed which immediately undergoes a second electron transfer at potentials of the original first wave. Lasia (17) recently reported the effect of alkali metal ions on the rate of dimerization of phthalic aldehyde radical anion in DMF solutions using cyclic voltammetric techniques. He showed that the rate of disappearance of the radical anion increased by several orders of magnitude in the presence of alkali metal ion, with tthe rate of disappearance following the order $Li^+ > Na^+ > K^+$.

The work described in this paper was undertaken to investigate the role of the alkali metal ion in the dimerization reaction of activated olefin radical anions and to ascertain if the reaction mechanism in the presence of these metal ions was the same as in their absence. A second purpose of this investigation, since information about the kinetics of the over-all process was to be obtained by chronocoulometric techniques, was to see if any adsorption of parent species or intermediates takes place. The previous investigations all assumed in their data treatment the absence of adsorption and the occurrence of the dimerization reaction away from the electrode surface. Although the fit of the experimental data to theoretical models not involving adsorption was very good, we felt that chronocoulometric techniques utilizing digital data acquisition (18, 19) would be a more sensitive probe of adsorption. We have recently shown using chronocoulometry (20), that neither 9,10-diphenylanthracene nor its radical anion are appreciably adsorbed in DMF solutions at a platinum electrode.

The substances investigated in this study were all activated olefins with the structure shown below

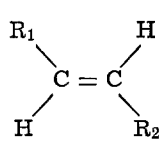

Dimethyl Fumarate:

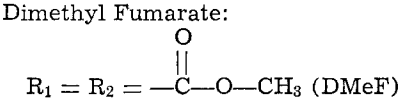

Diethyl Fumarate:

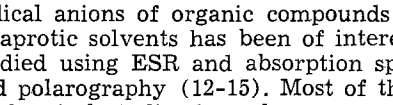

Dibutyl Fumarate:

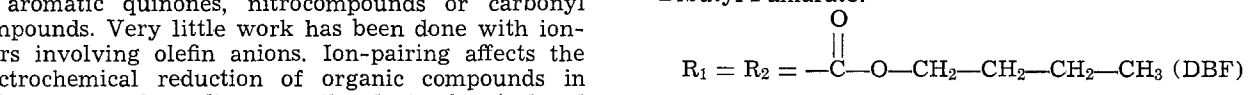

Ethyl Cinnamate:

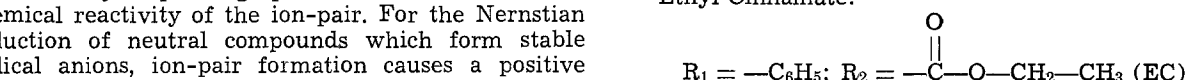

Cinnamonitrile:

$R_1 = -C_6H_5$; $R_2 = -CN$ (CN)

Fumaronitrile:

$R_1 = R_2 = -CN$ (FN)

Double potential step chronoamperometric and chronocoulometric data were fit to theoretical models produced by digital simulation techniques (2), to obtain rate constants of the reactions following electron transfer.

## Experimental

The general experimental techniques were the same as those reported previously (2); a detailed description is available (21).

*Materials.*—The solvent, dimethylformamide (DMF) (reagent grade, J. T. Baker Chemical Company) was purified by first storing over Linde Type 4A molecular sieves for 48 hr to remove the water, then storing over anhydrous cupric sulfate for 48 hr to complex dimethylamine. The solvent was then distilled from a small amount of molecular sieves and cupric sulfate using a 100 cm glass bead packed distillation column under a nitrogen atmosphere of 15 Torr using a reflux ratio of one. The middle 50% of the distillate was retained. This was stored under a helium atmosphere and used within three weeks of purification.

The supporting electrolyte, tetra-n-butylammonium iodide (TBAI) (polarographic grade, Southwestern Analytical Chemical Company, Austin, Texas) was vacuum dried and stored in a desiccator until use. Diethyl fumarate (DEF), cinnamonitrile (CN) (K. and K. Laboratories, Incorporated), and dibutyl fumarate (DBF) (Aldrich Chemical Company) were used as received. Dimethyl fumarate (K. and K. Laboratories, Incorporated) and fumaronitrile (FM) (Aldrich Chemical Company) were sublimed twice before use. Ethyl cinnamate (EC) (Aldrich Chemical Company) was vacuum distilled twice before use. Lithium perchlorate, lithium iodide, sodium iodide, and potassium iodide (reagent grade, J. T. Baker Chemical Company) were vacuum dried before use.

*Apparatus.*—The electrochemical cell used in the voltammetric studies was constructed from vacuum glassware and had a 25 ml capacity and contained a freeze-pump-thaw chamber and working, auxiliary, and reference electrode compartments. The auxiliary and reference electrode compartments were isolated from the working compartment by medium porosity glass frits. The cell contained four electrodes: a silver wire reference electrode, a platinum disk micro-electrode (0.013 $cm^2$) for chronocoulometry, chronoamperometry, and cyclic voltammetry, a platinum gauze macro-electrode for preelectrolysis, and a platinum coil auxiliary electrode. A second cell, similar to the cell described above, was used for controlled potential electrolysis. This cell had a 50 ml capacity and an intermediate chamber between the working and auxiliary compartments to prevent contamination of the working electrode compartment by diffusion of products produced at the auxiliary electrode during bulk controlled potential electrolysis. The working electrode

in the coulometric experiments was a platinum wire gauze (2 cm by 10 cm).

The silver wire reference electrode in TBAI-DMF solutions was reproducible (less than 10 mV deviation) and was stable for more than 24 hr (less than 5 mV drift). Its use avoided the water and KCl contamination that sometimes results from an aqueous SCE and also showed a smaller amount of a-c pickup than cells in which a conventional SCE was employed.

Cyclic voltammetry and controlled potential coulometry experiments were performed with a PAR Model 170 Electrochemistry System (Princeton Applied Research Corporation, Princeton, N.J.). Positive feedback resistance compensation was employed. Double potential step chronoamperometry and chronocoulometry experiments were performed with a multipurpose instrument constructed from solid-state operational amplifiers previously described (22-24), and also employed positive feedback resistance compensation (25). The potential step was applied to the summing point of the potentiostat by a Wavetek Model 114 Function Generator. The length of the potential step was measured with a Beckman Berkley Model 7370 Universal Eput and Timer. Initial and final potentials for the potential steps were measured with a Fairchild Model 7050 Digital Voltmeter to an accuracy of ± 1 mV.

Data for the potential step experiments were taken using a PDP-12A computer system (Digital Equipment Corporation, Maynard, Massachusetts) and generally followed previously described digital data acquisition techniques [see (21, 23, 24, 26-29) and references therein]. Data sampling by the computer was synchronized to the potential step by amplifying the potential step and using it to trigger the real-time clock of the computer. The real-time clock in turn initiated data sampling at a rate determined by the computer program. The PDP-12A data acquisition program allowed sampling of 50 data points on the forward pulse and 50 points on the reverse one. These could be displayed, subjected to an internal least squares routine in studies of adsorption, listed, or printed as $i(2t_f)/i(t_f)$ or $Q(2t_f)/Q(t_f)$ where $t_f$ is the forward pulse length, $i(t_f)$ and $Q(t_f)$ are the current and accumulated coulombs at $t_f$, respectively, and $i(2t_f)$ and $Q(2t_f)$ are these values at time $2t_f$.

*Typical experimental procedure.*—The platinum disk electrode was polished with AB ALPHA polishing alumina (Buehler Limited, Evanston, Illinois) before each experiment. The cell was assembled and pumped down on a vacuum line ($10^{-5}$ Torr) for 1-2 hr. The supporting electrolyte was vacuum-dried in a transfer vessel. DMF was then vacuum transferred to the transfer vessel containing the supporting electrolyte to give a volume of 25 or 50 ml. After the supporting electrolyte dissolved, the solution was subjected to three freeze-pump-thaw cycles to remove any traces of oxygen. The solution was then vacuum-transferred to the electrochemical cell, brought to atmospheric pressure with high purity helium (99.995% Matheson Gas Products, La Porte, Texas), and allowed to equilibrate for 1 hr.

Liquid olefins and concentrated solutions of alkali metal ions were then added to the electrochemical cell as needed through a septum cap with the aid of syringes. Solid olefins were generally added with the supporting electrolyte in the transfer vessel. Concentrated alkali metal ion solutions were prepared in a vacuum vessel in a manner similar to that of the supporting electrolyte solution, except, that the DMF was freeze-pump-thawed several times both before and after the addition of the metal iodides. This was done to prevent the possibility of air oxidation of iodide to iodine in the presence of metal ions such as lithium.

## Results

*Theoretical models.*—The method of obtaining kinetic and mechanistic information from the double potential step experiments generally followed that described previously (2). Briefly, digital simulations (30) of the current ($i$) and coulombs ($Q$) flowing during a potential step to the limiting current plateau of the first reduction wave (production of $R^{\cdot-}$, Eq. [2]) and of $i$ and $Q$ during a reverse step back to the foot of the wave (oxidation of $R^{\cdot-}$) were carried out, for different values of the rate constant of the dimerization reaction, Eq. [3]. For completeness, other possible reaction sequences leading from $R^{\cdot-}$ to hydrodimer were also considered; these are shown in Table I. Simulations employing 1000 iterations were used and tables of the normalized current and coulombs as functions of the dimensionless parameter $k_2t_fC$ were generated. These were then used to generate tables of $i(2t_f)/i(t_f)$ and $Q(2t_f)/Q(t_f)$ as functions of $k_2t_fC$. To fit the experimental data to the models, it is convenient to normalize these current and coulomb ratios and to represent these ratios as functions of a particular time when these ratios attain a certain value. The normalized ratios were obtained, as previously (2), *i.e.*

$$R_I = [i(2t_f)/i(t_f)]/0.2928 \quad [5]$$

$$R_Q = \frac{[Q(2t_f)/Q(t_f)] - 0.414}{0.586} \quad [6]$$

so that $R_I$ is 1 and $R_Q$ is 0 in the absence of kinetic complications ($k_2 = 0$), with $R_I$ decreasing to 0 and $R_Q$ increasing to 1 for very large values of $k_2t_fC$. In our previous work (2) we picked as the time reference point that value of $k_2t_fC$ where $R_I = 0.5$, calling this point $t_{1/2}$ and using plots of $R_I$ and $R_Q$ *vs.* $t_{1/2}$ to determine the mechanism and the rate constant. Because we make greater use of the $R_Q$ curves in the present work, we found it more convenient (and somewhat more diagnostic since the curves for the different possible mechanisms were more spread apart) to use as a reference point that where $R_Q = 0.4$; this value of $k_2t_fC$ is designated as $T_{Q.4}$. A plot of $R_I$ and $R_Q$ *vs.* $T_{Q.4}$ is shown in Fig. 1 and, as an aid for others desiring to

**Table I. $R(Q)$ and $R(I)$ vs. $T_{Q.4}$ (up to eight $T_{Q.4}$ values) for four possible electrohydrodimerization mechanisms[a]**

| $T/T_{0.4}$ | Mechanism 1 $R(Q)$ | Mechanism 1 $R(I)$ | Mechanism 2 $R(Q)$ | Mechanism 2 $R(I)$ | Mechanism 3 $R(Q)$ | Mechanism 3 $R(I)$ | Mechanism 4 $R(Q)$ | Mechanism 4 $R(I)$ |
|---|---|---|---|---|---|---|---|---|
| 0.00 | 0.000 | 1.000 | 0.000 | 1.000 | 0.000 | 1.000 | 0.000 | 1.000 |
| 0.30 | 0.179 | 0.778 | 0.173 | 0.635 | 0.168 | 0.633 | 0.180 | 0.858 |
| 0.50 | 0.262 | 0.680 | 0.256 | 0.488 | 0.252 | 0.485 | 0.261 | 0.790 |
| 0.80 | 0.354 | 0.575 | 0.350 | 0.338 | 0.350 | 0.337 | 0.352 | 0.711 |
| 1.00 | 0.401 | 0.522 | 0.400 | 0.269 | 0.401 | 0.269 | 0.399 | 0.669 |
| 1.30 | 0.461 | 0.459 | 0.462 | 0.192 | 0.468 | 0.196 | 0.453 | 0.619 |
| 1.60 | 0.504 | 0.413 | 0.511 | 0.139 | 0.521 | 0.145 | 0.497 | 0.576 |
| 2.00 | 0.551 | 0.364 | 0.565 | 0.091 | 0.577 | 0.099 | 0.542 | 0.532 |
| 2.40 | 0.588 | 0.326 | 0.607 | 0.061 | 0.622 | 0.069 | 0.577 | 0.496 |
| 2.80 | 0.618 | 0.296 | 0.642 | 0.040 | 0.659 | 0.049 | 0.605 | 0.467 |
| 3.20 | 0.643 | 0.271 | 0.671 | 0.027 | 0.689 | 0.035 | 0.629 | 0.442 |
| 3.60 | 0.664 | 0.250 | 0.695 | 0.018 | 0.715 | 0.025 | 0.647 | 0.422 |
| 4.00 | 0.683 | 0.233 | 0.716 | 0.012 | 0.737 | 0.018 | 0.664 | 0.403 |
| 4.40 | 0.698 | 0.218 | 0.733 | 0.008 | 0.755 | 0.013 | 0.678 | 0.387 |
| 4.80 | 0.712 | 0.205 | 0.749 | 0.006 | 0.772 | 0.010 | 0.690 | 0.374 |
| 5.20 | 0.725 | 0.193 | 0.763 | 0.004 | 0.786 | 0.007 | 0.701 | 0.361 |
| 5.60 | 0.736 | 0.183 | 0.775 | 0.003 | 0.798 | 0.005 | 0.710 | 0.350 |
| 6.00 | 0.746 | 0.174 | 0.785 | 0.002 | 0.809 | 0.004 | 0.719 | 0.340 |
| 6.40 | 0.754 | 0.166 | 0.795 | 0.001 | 0.819 | 0.003 | 0.726 | 0.331 |
| 6.90 | 0.765 | 0.157 | 0.805 | 0.001 | 0.830 | 0.002 | 0.734 | 0.321 |
| 7.50 | 0.775 | 0.147 | 0.816 | 0.000 | 0.842 | 0.001 | 0.743 | 0.311 |
| 8.00 | 0.783 | 0.140 | 0.824 | 0.000 | 0.850 | 0.001 | 0.750 | 0.302 |

[a] Mechanism 1. Second order dimerization [Mechanism V in (2)]

At $E_1$: $R + e \rightarrow R^{\cdot-}$ $\quad 2R^{\cdot-} \xrightarrow{k_2} R_2^{2-}$
At $E_2$: $R^{\cdot-} \rightarrow R + e$

Mechanism 2. Second order EC [Mechanism III in (2)]

At $E_1$: $R + 2e \rightarrow R^{2-}$ $\quad R^{2-} + R \xrightarrow{k_2} R_2^{2-}$
At $E_2$: $R^{2-} \rightarrow R + 2e$

Mechanism 3. Second order ECE [Mechanism IV in (2)]

At $E_1$: $R + e \rightarrow R^{\cdot-}$ $\quad R^{\cdot-} + R \xrightarrow{k_2} R_2^{\cdot-}$
At $E_2$: $R^{\cdot-} \rightarrow R + e$

Mechanism 4. Second order ECE [Mechanism IVA in (2)]

As Mechanism 3, except:
At $E_2$: $R^{\cdot-} \rightarrow R + e$
$R_2^{\cdot-} \rightarrow$ products $+ e$

Rate constants for each mechanism can be calculated by the following equations: Mechanism 1, $k_2 = 0.755/T_{Q.4}C$; Mechanism 2, $k_2 = 1.92/T_{Q.4}C$; Mechanism 3, $k_2 = 1.45/T_{Q.4}C$; Mechanism 4, $k_2 = 3.86/T_{Q.4}C$.

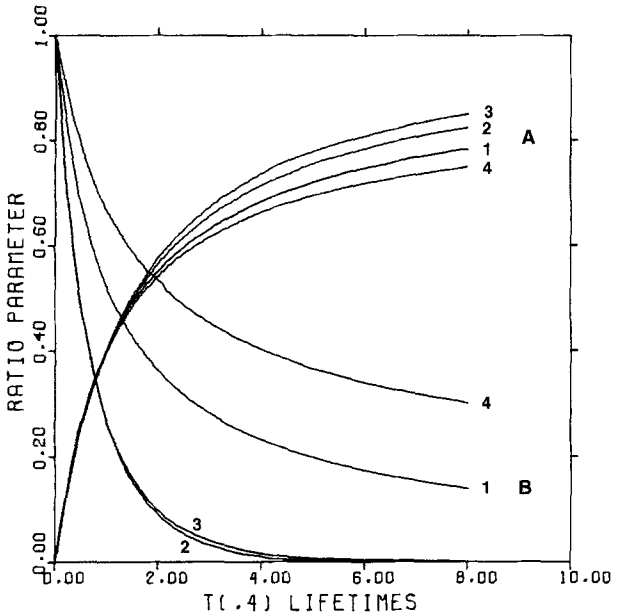


**Fig. 1. Variation of the normalized coulomb (A) and current (B) ratio parameters as a function of $T_{Q.4}$ lifetimes for the different mechanisms considered.**

use this procedure, the data is tabulated in Table I. In use the experimental $R_I$ and $R_Q$ values are plotted against $t_f$, and the time axis then recalibrated in terms of $T_{Q.4}$ values. The fit of the experimental curve to the different model curves reveals the best mechanism, and the $T_{Q.4}$ value for that mechanism, knowing $t_f$ and C, yields $k_2$ (Table I).

*Models in the presence of alkali metal ions.*—The results show (see below) that the hydrodimerization mechanism involves coupling of the radical anions (Mechanism 1) even in the presence of alkali metal ions. The involvement of alkali metal ion could proceed by ion pair formation, followed by reaction of ion pair with free radical anion

$$R^{\cdot-} + M^+R^{\cdot-} \xrightarrow{k_{21}} \text{dimer} \qquad [7]$$

or by coupling of two ion pairs

$$2\,M^+R^{\cdot-} \xrightarrow{k_{22}} \text{dimer} \qquad [8]$$

If one assumes that these are the rate-determining steps, *i.e.*, that ion pair formation and dissociation are so rapid, that reaction [9] can be considered at equilibrium

$$M^+ + R^{\cdot-} \rightleftarrows M^+\,R^{\cdot-} \qquad [9]$$

the over-all reaction velocity for the two paths can be obtained by combining the equilibrium constant expression for [9] (Eq. [10])

$$K = [M^+R^-]/[M^+][R^{\cdot-}] \qquad [10]$$

with the rate expressions for [7] and [8]

$$v_7 = k_{21}[R^{\cdot-}][M^+R^{\cdot-}] \qquad [11]$$

$$v_8 = k_{22}[M^+R^{\cdot-}]^2 \qquad [12]$$

Taking the analytical concentration of radical anion as $C_{R^{\cdot-}}$ (Eq. [13]), the concentration of ion pair

$$C_{R^{\cdot-}} = [R^{\cdot-}] + [M^+R^{\cdot-}] \qquad [13]$$

is given by Eq. [14]

$$[M^+R^{\cdot-}] = \frac{K[M^+]}{1 + K[M^+]}\,C_{R^{\cdot-}} \qquad [14]$$

and that of the free radical ion by Eq. [15]

$$[R^{\cdot-}] = C_{R^{\cdot-}}/(1 + K[M^+]) \qquad [15]$$

Using these expressions in Eq. [11] and [12] yield

$$v_7 = \frac{k_{21}K[M^+]}{(1 + K[M^+])^2}\,C_{R^{\cdot-}}{}^2 \qquad [16]$$

$$v_8 = \frac{k_{22}K^2[M^+]^2}{(1 + K[M^+])^2}\,C_{R^{\cdot-}}{}^2 \qquad [17]$$

Both mechanisms show an over-all second order dependence on total radical anion concentration. The dependence on free metal ion concentration, in the limit $K[M^+] << 1$ (where Eq. [18] and [19] apply) is first order

$$v_7 = k_{21}K[M^+]\,C_{R^{\cdot-}}{}^2 \qquad [18]$$

$$v_8 = k_{22}K^2[M^+]^2\,C_{R^{\cdot-}}{}^2 \qquad [19]$$

for the reaction in [7] and second order for that in [8]. The general over-all equation for the reaction rate under conditions where free radical ion coupling, and the ion-pair coupling reactions can all occur simultaneously is given by

$$v_{\text{over-all}} = \frac{k_2 + k_{21}K[M^+] + k_{22}K^2[M^+]^2}{(1 + K[M^+])^2}\,C_{R^{\cdot-}}{}^2 \qquad [20]$$

*Electrochemical results in absence of alkali metal ions.*—Cyclic voltammetric data for the different activated olefins are given in Table II. All compounds show behavior typical of a one-electron transfer followed by a following chemical reaction. In all cases the voltammograms become more reversible in appearance (*e.g.*, show larger $i_{pa}/i_{pc}$-values) when either the scan rate is increased or the olefin concentration is decreased. In general the results for DEF and CN confirm those in earlier papers (2-3). Controlled potential coulometric reduction of these compounds was carried out at potentials beyond the first reduction peak; typical results are given in Table III. For the fumarates all show $n_{app}$-values smaller than one, with $n_{app}$-values smaller at higher (10 m*M*) concentrations than at lower (2.0 m*M*) ones. This has been attributed to a slow polymerization reaction initiated by the radical anions. For both EC and CN the $n_{app}$-values are much closer to one, suggesting considerably less polymerization occurs with these species.

**Table II. Cyclic voltammetry results for activated olefins in absence of alkali metal ions[a]**

| Compound | Conc (mM) | $E_{pc}$ (V. *vs.* Ag.R.E.) | $E_{pc} - E_{pc/2}$ (mV) | $\frac{i_{pc}}{v^{1/2}\,C}$ $\frac{\mu A - sec^{1/2}}{V - mM}$ | $E_{pc} - E_{pa}$ (mV) | $\frac{i_{pa}}{i_{pc}}$ |
|---|---|---|---|---|---|---|
| DBF | 1.49 | −0.83 | 65 | 8.7 | 80 | 0.84 |
| DEF | 2.00 | −0.82 | 60 | 9.3 | 85 | 0.73 |
| DMeF | 3.00 | −0.78 | 63 | 10.9 | 80 | 0.50 |
| EC | 1.80 | −1.25 | 70 | 9.9 | 90 | 0.60 |
| CN | 2.33 | −1.25 | 61 | 10.9 | 80 | 0.41 |

[a] All solutions were 0.20*M* TBAI in DMF with scan rate ($v$) of 200 mV/sec.

**Table III. Controlled potential coulometry results for the reduction of activated olefins[a]**

| Compound | Conc (mM) | $E_{appl}$ (V. *vs.* Ag.R.E.) | $n_{app}$ |
|---|---|---|---|
| DBF | 2.00 | −1.00 | 0.80 |
| | 10.7 | −1.00 | 0.55 |
| DEF | 2.00 | −1.00 | 0.85 |
| | 10.0 | −1.00 | 0.60 |
| DMeF | 2.0 | −1.00 | 0.82 |
| | 10.0 | −1.00 | 0.63 |
| EC | 2.0 | −1.40 | 0.96 |
| | 10.3 | −1.40 | 0.91 |
| CN | 1.0 | −1.40 | 0.99 |
| | 11.0 | −1.40 | 0.82 |

[a] 0.20*M* TBAI-DMF at Pt cathode.

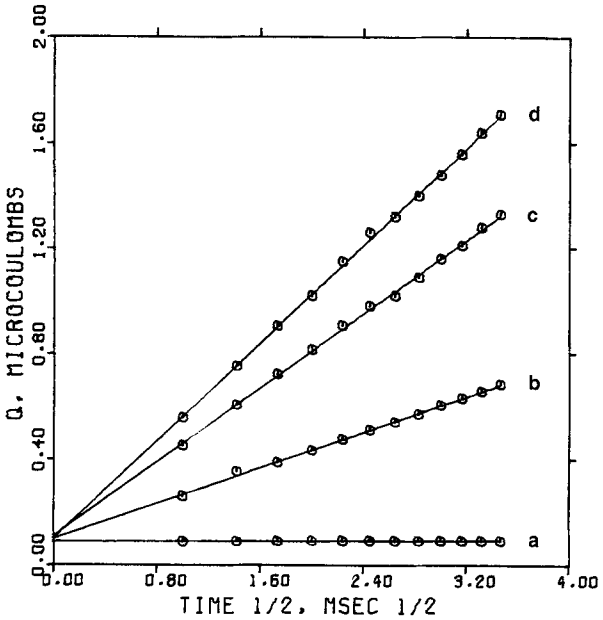


Fig. 2. Chronocoulometric data ($Q$ vs. $t^{1/2}$) for dibutyl fumarate. The potential was stepped from −0.200 to −1.000V vs. AgR.E. and the solution was 0.2M TBAI in DMF containing (a) 0, (b) 1.49, (c) 3.20, (d) 4.11 mM DBF.

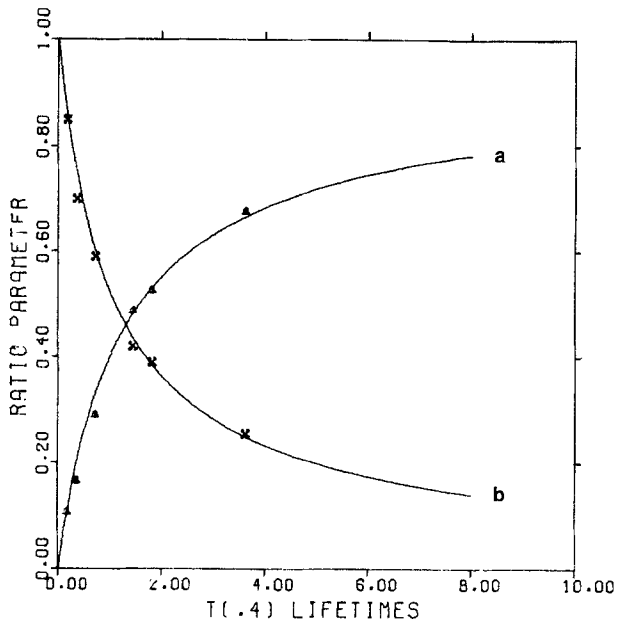


Fig. 3. Variation of the normalized coulomb (a) and current (b) ratio parameters as a function of $T_{Q.4}$ lifetimes for the reduction of 20.4 mM dibutyl fumarate in 0.20M TBAI-DMF solution. The points are experimental data and the lines are the simulation results for Mechanism 1 (radical anion dimerization).

Potential step chronocoulometry from the foot of the wave to the mass transfer limiting region in all cases produced linear $Q$ vs. $t^{1/2}$ plots. Typical results are shown in Fig. 2; complete data are in Ref. (21). The intercepts and slopes for all of the compounds at several concentrations are given in Table IV. Analysis of the chronocoulometric data by the equation (18-20)

$$Q = Q_{dl} + n\mathbf{F}A\Gamma + 2n\mathbf{F}AC(D_o t/\pi)^{1/2} \qquad [21]$$

shows that the intercept at $C = 0$ is the same as at higher concentrations of electroactive species, within ±0.01 μC. The maximum amount of adsorbed electroactive species is thus about 0.77 μC/cm² or $8 \times 10^{-12}$ mole/cm²; this corresponds to a maximum electrode coverage of 2-3%. The slopes are proportional to C in all cases. The linearity of the $Q$ vs. $t^{1/2}$ plots also indicates that polymerization is not important during the duration of the chronocoulometric experiment, since any appreciable extent of polymerization would consume parent species and lead to a nonlinear plot.

Table IV. Chronocoulometric $Q$ vs. $t^{1/2}$ intercepts and slopes[a]

| Concentration (mM) | Intercept (μC) | Slope (μC/msec$^{1/2}$) | Slope/C (μC msec$^{-1/2}$/mM) |
|---|---|---|---|
| Dibutyl fumarate ($E_i$ = −0.20V, $E_f$ = −1.00V) | | | |
| 0 | 0.094 | 0.002 | |
| 1.49 | 0.100 | 0.169 | 0.113 |
| 3.20 | 0.112 | 0.350 | 0.109 |
| 4.11 | 0.101 | 0.463 | 0.112 |
| Diethyl fumarate ($E_i$ = 0.40V, $E_f$ = −1.00V) | | | |
| 0 | 0.083 | 0.002 | |
| 1.02 | 0.083 | 0.123 | 0.121 |
| 2.24 | 0.087 | 0.276 | 0.123 |
| 3.47 | 0.086 | 0.439 | 0.126 |
| Dimethyl fumarate ($E_i$ = −0.40V, $E_f$ = −1.00V) | | | |
| 0 | 0.087 | 0.002 | |
| 1.10 | 0.089 | 0.140 | 0.127 |
| 3.00 | 0.084 | 0.395 | 0.131 |
| 5.00 | 0.101 | 0.583 | 0.117 |
| Ethyl cinnamate ($E_i$ = −0.80V, $E_f$ = −1.40V) | | | |
| 0 | 0.082 | 0.001 | |
| 0.85 | 0.089 | 0.098 | 0.115 |
| 1.79 | 0.084 | 0.207 | 0.115 |
| Cinnamonitrile ($E_i$ = −0.40V, $E_f$ = −1.40V) | | | |
| 0 | 0.160 | 0.003 | |
| 1.54 | 0.160 | 0.210 | 0.136 |
| 3.12 | 0.159 | 0.389 | 0.125 |
| 4.80 | 0.152 | 0.544 | 0.113 |
| 6.41 | 0.170 | 0.738 | 0.115 |

[a] Solutions were 0.20M TBAI in DMF. $E_i$ is the initial potential and $E_f$ the final potential, in V vs. Ag.R.E.

Mechanistic information was obtained by double potential step chronocoulometry and chronoamperometry, using the variation of $Q(2t_f)/Q(t_f)$ and $i(2t_f)/i(t_f)$ with the duration of the potential step, $t_f$, to obtain the ratio parameters $R_Q$ and $R_I$ and the $T_{Q.4}$-value. These experimental $R_Q$ and $R_I$ vs. $T_{Q.4}$ curves were compared to the theoretical ones (Fig. 1) to establish the mechanism and determine the rate constant. Typical experimental data for DBF compared to theoretical curves for Mechanism 1 are shown in Fig. 3. The experimental values for the other compounds show essentially an equally good fit to Mechanism 1; complete data and curves are available (21). The experimental rate constants obtained for the dimerization from this data are listed in Table V. For those that have been determined before (DEF, DMeF, CN) (2-5), the results here are in good agreement with previously reported values.

*Electrochemical results in the presence of alkali metal ions.*—Addition of alkali metal salts causes the cyclic voltammograms for the reduction of the olefins to change—$E_{pc}$ shifts slightly in a positive direction and $i_{pa}/i_{pc}$ is decreased; typical results are shown in Fig. 4. The positive shift in $E_{pc}$ is in the order $Li^+ > Na^+ > K^+$, and can be attributed to ion pair formation of the radical anion with the metal ion and an increased rate of the following dimerization reaction. The current functions $i_{pc}/v^{1/2}C$ were similar to those without alkali metal ions and they decreased slightly with increasing scan rate. The anodic peak current, $i_{pa}$, was much smaller with alkali metal ions present, indicating a much faster following chemical reaction. For a given scan rate and metal ion concentration, the voltammograms showed larger $i_{pa}/i_{pc}$ ratios when the olefin concentration was decreased, indicating a higher order following chemical reaction. For a given cyclic voltammetric scan rate, concentration of olefin, and concentration of metal ion, $i_{pa}/i_{pc}$ increased in the order $Li^+ < Na^+ < K^+$. Thus the rate of the dimerization reaction is in the order $Li^+ > Na^+ > K^+ >$ no added alkali metal ion.

Controlled potential coulometry experiments were performed on solutions of dimethyl fumarate, diethyl fumarate, dibutyl fumarate, ethyl cinnamate, cinna-

**Table V. Rate constants for dimerization of several activated olefins obtained from double potential step chronoamperometric and chronocoulometric measurements[a]**

| | Concentration (mM) | $T_{0.4}$ (sec) | $k_2$ (l/mole-sec) |
|---|---|---|---|
| Dibutyl fumarate | 1.49 | 20.0 | 25 |
| | 10.1 | 3.30 | 24 |
| | 15.1 | 2.17 | 23 |
| | 20.4 | 1.38 | 26 |
| | | | Avg = 25 |
| Diethyl fumarate | 7.0 | 2.30 | 47 |
| | 10.0 | 1.68 | 43 |
| | 10.0 | 1.66 | 44 |
| | 21.4 | 0.83 | 42 |
| | | | Avg = 44 |
| Dimethyl fumarate | 3.00 | 2.07 | $1.2 \times 10^2$ |
| | 5.0 | 1.35 | 1.1 |
| | 10.0 | 0.62 | 1.2 |
| | | | Avg = $1.2 \times 10^2$ |
| Ethyl cinnamate | 3.69 | 1.46 | $1.4 \times 10^2$ |
| | 5.55 | 0.905 | 1.5 |
| | 7.43 | 0.710 | 1.4 |
| | 9.26 | 0.585 | 1.4 |
| | | | Avg = $1.4 \times 10^2$ |
| Cinnamonitrile | 1.26 | 0.673 | $8.9 \times 10^2$ |
| | 1.56 | 0.581 | 8.4 |
| | 1.88 | 0.455 | 8.8 |
| | 2.33 | 0.365 | 8.9 |
| | 3.78 | 0.223 | 8.9 |
| | 5.18 | 0.166 | 8.8 |
| | 5.82 | 0.152 | 8.5 |
| | 7.79 | 0.108 | 9.0 |
| | | | Avg = $8.77 \times 10^2$ |

[a] 0.2*M* TBAI in DMF; potential step program $E_i \rightarrow E_f \rightarrow E_i$ as in Table IV.

monitrile, and fumaronitrile in 0.20*M* TBAI-DMF with $Li^+$, $Na^+$, and $K^+$ ions added. Olefin concentrations ranged from 2.0 to 15.0 mM, while alkali metal ion ($M^+$) to olefin ratios up to ten to one were used. Typical $n_{app}$-values for solutions with 10 mM olefin and various $[M^+]$/[olefin] ratios are shown in Table VI.

Experiments involving DBF, DEF, and DMeF with $Li^+$ added to the solution gave an $n_{app}$ of $1.00 \pm 0.03$ when the $[Li^+]$/[olefin] ratio was greater than four. The $n_{app}$ decreased to the value obtained in the absence of alkali metal ion when the $[Li^+]$/[olefin] ratio decreased. Experiments using LiI, $LiClO_4$, and $LiClO_4 \cdot 3H_2O$ as the source of $Li^+$ all gave essentially the same $n_{app}$ values. The electrolysis times of the anhydrous solutions containing alkali metal ions were 10-25% longer than the same solutions lacking $M^+$ under the same electrolysis conditions. Solutions with

**Table VI. Typical controlled potential coulometry results for reduction of several activated olefins in the presence of $Li^+$, $Na^+$, or $K^+$[a]**

| | $n_{app}$ values DBF | DEF | DMeF | Fumaronitrile |
|---|---|---|---|---|
| [$Li^+$]/[olefin] | | | | |
| 6.0 | 0.98 | 1.02 | 0.97 | 0.43 |
| 4.0 | 1.00 | 0.99 | 0.99 | |
| 3.0 | 0.90 | 0.96 | 0.94 | |
| 2.0 | 0.89 | 0.91 | 0.91 | |
| 1.0 | 0.81 | 0.84 | 0.86 | |
| 0.0 | 0.55 | 0.60 | 0.63 | 0.41 |
| [$Na^+$]/[olefin] | | | | |
| 10.0 | 0.53 | 0.63 | 0.60 | 0.37 |
| 4.0 | 0.57 | 0.59 | 0.59 | |
| [$K^+$]/[olefin] | | | | |
| 10.0 | 0.58 | 0.62 | 0.64 | 0.42 |
| 4.0 | 0.57 | 0.65 | 0.61 | |

[a] All solutions were 10.0 mM in olefin in 0.20*M* TBAI-DMF solution.

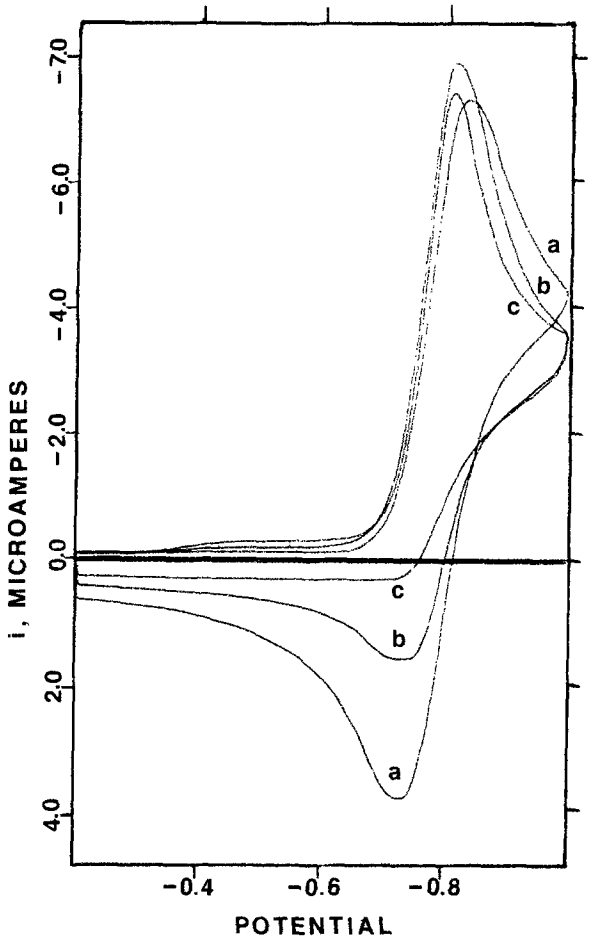


**Fig. 4. Effect of $Na^+$ on the cyclic voltammetry of diethyl fumarate. The scan rate was 100 mV/sec and the DMF solution contained 0.20M TBAI, 1.49 mM DEF, and (a) 0, (b), 1.00 mM, (c) 12.0 mM NaI.**

$n_{app}$-values close to one were colorless after the electrolysis, while solutions with $n_{app}$-values less than one had a yellow-brown color. During electrolysis with $Li^+$ present, a continuous formation of small bubbles was observed on the working electrode; the amount of these bubbles increased with increasing $Li^+$ concentration and were much more prevalent in the anhydrous solutions.

The $n_{app}$-values for the reduction of DMeF, DEF, and DBF were essentially unaffected by addition of $Na^+$ or $K^+$, even with $[Na^+]$ or $[K^+]$ to [olefin] ratios of 10/1 (film formation with DBF — $K^+$ solutions prevented an exhaustive electrolysis). Solutions containing $Na^+$ and $K^+$ were also characterized by a yellow-brown color after the electrolysis. The electrolysis times for solutions containing $Na^+$ and $K^+$ were three to five times longer than for solutions which did not contain alkali metal ions. We believe that a film of alkali metal hydroxide is formed during the electrolysis which partially blocks the electrode surface. This arises because the small hydrogen ion concentration that is present in solution is depleted in the vicinity of the electrode surface by the hydrodimerization reaction. When a small amount of water (0.1 ml per 50 ml DMF) was added as a weak proton source, the electrolysis times were reduced approximately 20%; however, they were still longer than the electrolysis times for solutions where no alkali metal ions were present. The water did not affect the $n_{app}$-values, but it did substantially increase the background current after electrolysis.

An NMR analysis was carried out on the electrolysis products for the reduction of DEF with $Li^+$ ($[Li^+]$/[DEF]) = 4.0 and $K^+$ ($[K^+]$/[DEF] = 6.0) present. The NMR analysis could not be performed directly

on the electrolysis solution since the NMR spectra of the DMF and TBAI completely obscured the spectra of the electrolysis products. It was therefore necessary to extract the electrolysis products into methylene chloride, evaporate the methylene chloride and then obtain the NMR spectrum in carbon tetrachloride. The NMR of the electrolysis products were compared with those of pure samples of the hydrodimer (generously provided by Dr. M. Baizer of Monsanto, St. Louis, Missouri), diethyl succinate, and diethyl fumarate after they had undergone the same extraction process as the electrolysis products. The NMR spectrum of the $Li^+$ DEF electrolysis product was very similar to that of the pure hydrodimer, (1,2,3,4-tetraethyl butane tetracarboxylate); the electrolysis products, showed a small peak from unelectrolyzed DEF remaining in solution, and peaks from DMF carried over in the extraction. No singlet peak was observed at 7.50 $\tau$, indicating that no dihydro product (diethyl succinate), was formed during the electrolysis. The NMR of the $K^+$-DEF electrolysis products gave spectra similar to that of the hydrodimer; however, each of the major peaks were split indicating several similar, but different, electrolysis products (*e.g.*, hydrodimer and polymer). When the $K^+$-DEF electrolysis products were vacuum distilled at 120°C, the distillate was a clear liquid (giving a hydrodimer NMR spectrum) while a brown tar remained in the distillation pot. The NMR spectrum of the brown tar exhibited the same number of peaks as the hydrodimer with slightly different chemical shifts. The NMR and $n_{app}$ data indicate, in agreement with our previous results (2), that the polymerization reaction is eliminated and the hydrodimer becomes the only major electrolysis product upon addition of lithium ion, while, both sodium and potassium ions have no effect on the distribution of the final electrolysis products.

Electrolysis experiments were also carried out with fumaronitrile ($E_{pc} = -0.72$V *vs.* AgR.E.) to see if alkali metal ions affected its reduction products in a manner similar to that for the fumarates. The $n_{app}$ in the absence of alkali metal ions was found to be approximately 0.40, which indicates that a polymerization reaction involving parent molecules occurs. In this case the addition of $Li^+$, $Na^+$, or $K^+$ had no effect on the $n_{app}$-value. The electrolyses of cinnamonitrile and ethyl cinnamate were obscured by electrode filming and the electrochemical reduction of the metal ions to metal.

The experimental results for potential step chronocoulometry are summarized in Table VII; typical $Q - t^{1/2}$ curves in the absence and presence of LiI and DBF are shown in Fig. 5. The addition of alkali metal iodide causes the intercept to increase above that characteristic of the 0.2*M* TBAI-DMF solution. If we assume that there is no specific adsorption of cation at the initial potential (0.00V), then this increase can be attributed to rapid adsorption of the alkali metal ion at −1.00V requiring additional (negative) charge to compensate for these adsorbed positive ions. Under these conditions the relative extent of adsorption of alkali metal ion follows the order $K^+ > Na^+ > Li^+$.[1] The intercepts with the olefins present were essentially the same as those in their absence, indicating no appreciable adsorption of DBF and DEF.

Chronocoulometric $Q$ *vs.* $\theta$ plots for the reverse potential step, while slightly perturbed by the hydrodimerization reaction, gave intercepts close to the value (±0.04 $\mu$C) obtained for the forward step both in the absence and presence of DBF and DEF for all three alkali metal ions. This indicates that neither the radical anions produced nor any metal ion-radical anion ion-pair formed is appreciably adsorbed on the electrode surface.

[1] Another interpretation of the results, suggested by a reviewer, is adsorption of alkali metal ion at the initial potential which leads, through cooperative adsorption, to even greater adsorption of $I^-$ and an initial increase in positive charge on the electrode.

**Table VII. Chronocoulometric $Q - t^{1/2}$ intercepts and slopes[a]**

| Olefin conc (m*M*) | Alkali metal ion conc (mM) | Intercept ($\mu$C) | Slope ($\mu$C/msec$^{1/2}$) |
|---|---|---|---|
| Dibutyl fumarate | LiI | | |
| 0 | 0 | 0.17 | 0.000 |
| 0 | 1.00 | 0.25 | 0.001 |
| 1.69 | 1.00 | 0.25 | 0.158 |
| 3.40 | 7.90 | 0.26 | 0.308 |
| Dibutyl fumarate | NaI | | |
| 0 | 1.00 | 0.481 | 0.003 |
| 1.99 | 1.00 | 0.486 | 0.238 |
| 3.00 | 21.8 | 0.508 | 0.356 |
| Dibutyl fumarate | KI | | |
| 0 | 1.00 | 0.602 | 0.003 |
| 1.50 | 1.00 | 0.605 | 0.154 |
| 3.20 | 11.1[b] | 0.465 | 0.222 |
| Diethyl fumarate | LiI | | |
| 0 | 1.00 | 0.253 | 0.003 |
| 1.13 | 1.00 | 0.256 | 0.160 |
| 2.01 | 4.41 | 0.248 | 0.306 |
| Diethyl fumarate | NaI | | |
| 0 | 1.00 | 0.481 | 0.004 |
| 1.49 | 1.00 | 0.492 | 0.179 |
| 2.94 | 8.00 | 0.509 | 0.352 |
| Diethyl fumarate | KI | | |
| 0 | 1.13 | 0.609 | 0.002 |
| 3.32 | 8.77 | 0.618 | 0.398 |
| 6.02 | 12.9 | 0.629 | 0.763 |

[a] Solutions were 0.20*M* TBAI in DMF. $E_i = 0.000$V and $E_f = -1.000$V *vs.* AgR.E.
[b] Electrode filming occurred in DBF-KI solutions under these conditions.

Information about the reaction mechanism in the presence of alkali metal ions was again obtained by double potential step chronocoulometry and chronoamperometry, using the experimental $R_Q$, $R_I$, and $T_{Q,4}$-values to test theoretical models and obtain rate constants. Even in the presence of alkali metal ions, the results for reduction of DEF and DBF show the best fit with Mechanism 1 (dimerization of radical anions); typical experimental results are shown in Fig. 6. The over-all rate constants, $k_{obs}$, for the dimerizations as calculated from these results for different olefin and alkali metal ion concentrations are given in Table VIII. The reaction order with respect to alkali metal ion concentration was first estimated

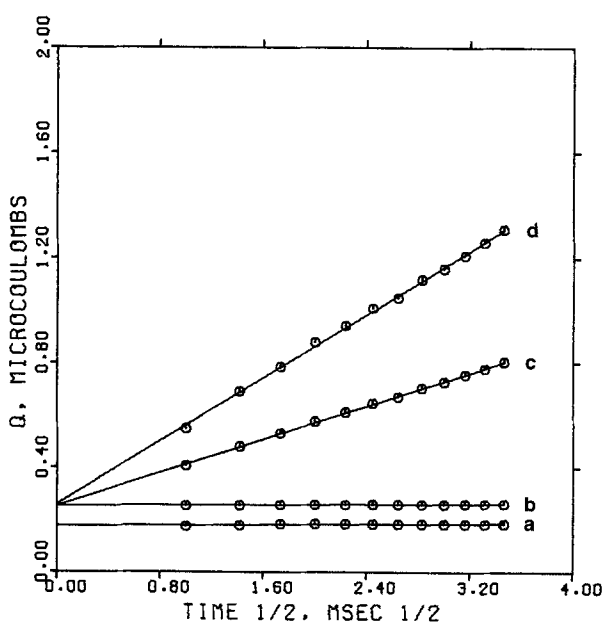


**Fig. 5. Chronocoulometric data ($Q$ *vs.* $t^{1/2}$) for dibutyl fumarate. The potential was stepped from 0.00 to −1.000V *vs.* AgR.E. and the DMF solution contained 0.20M TBAI and (a) 0 DBF, 0 LiI; (b) 0 DBF, 1.00 mM LiI; (c) 1.69 mM DBF, 1.00 mM LiI; (d) 3.40 mM DBF, 7.90 mM LiI.**

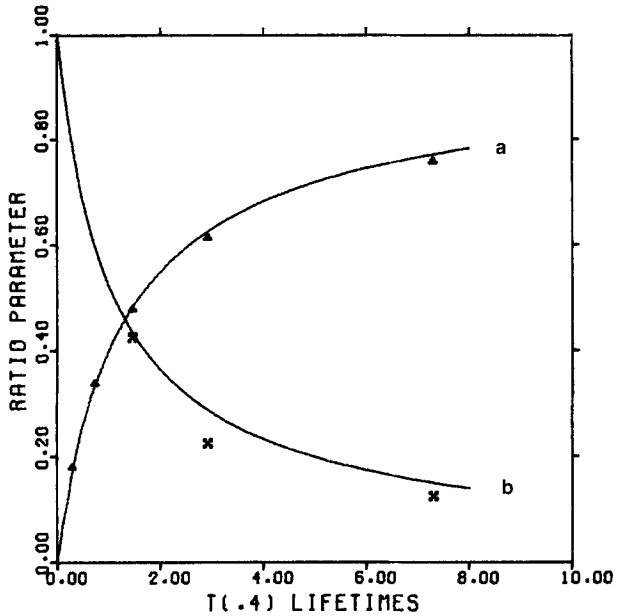


Fig. 6. Variation of the normalized coulomb (a) and current (b) ratio parameters as a function of $T_{Q.4}$ lifetimes for the reduction of 0.95 mM diethyl fumarate with 3.81 mM LiI in 0.20M TBAI-DMF solution. The points are experimental data and the lines are the simulation results for Mechanism 1 (radical anion dimerization).

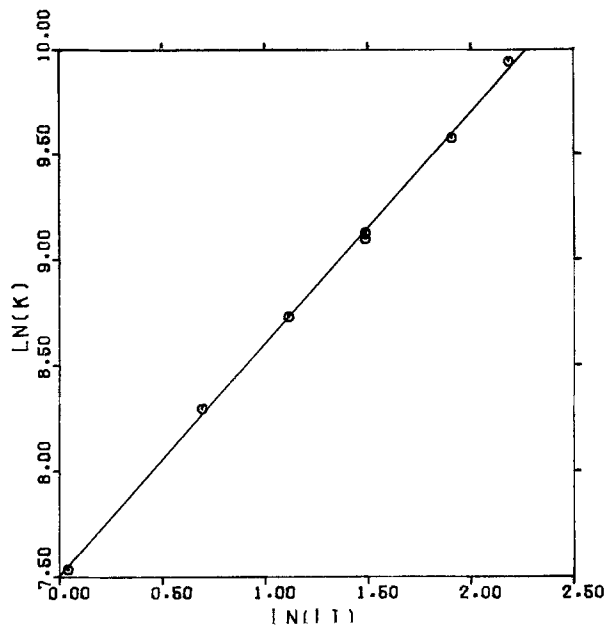


Fig. 7. Variation of ln $k_{obs}$ with ln [$Li^+$] for the electroreduction of diethyl fumarate in 0.20M TBAI-DMF.

by plotting ln $k_{obs}$ against ln [$M^+$]; a typical plot is shown in Fig. 7. The slopes of these plots, *i.e.*, the over-all reaction orders, using the data in Table VIII are for DEF : $Li^+$, 1.08 ± 0.02; $Na^+$, 1.07 ± 0.04; $K^+$, 0.89 ± 0.03 and for DBF : $Li^+$, 1.11 ± 0.03; $Na^+$, 0.85 ± 0.03. At ratios of $M^+$ to olefin less than 0.8, a larger deviation from first order dependence on $M^+$ was observed, because of the contribution to the over-all rate by the direct dimerization of the radical ions. Since the reactions were close to first order, the reaction mechanism most closely followed Eq. [7] and the appropriate kinetic expression is [16] or [18]. Thus the over-all rate constant, $k_{obs}$, is approximately $k_{21}K[M^+]$; the values of $k_{obs}/[M^+] \simeq k_{21}K$ given in Table VIII are fairly constant, as expected. The ion-pair formation constant for $DEF^{\cdot-}$ with $Li^+$, $Na^+$, and $K^+$ cations was estimated by the cyclic voltammetric potential shifts on the DEF reduction wave with the addition of alkali metal ions. The observed potential shifts are a result of both ion-pairing and the increased dimerization rate. The potential shift due to the hydrodimerization reaction can be estimated by using the theory of cyclic voltammetry in the presence of a dimerization reaction (6, 31) and the rate constant calculated by chronocoulometry. Once this has been calculated, the shift due to ion-pairing can be extracted, and the ion-pair formation constant is then estimated using Eq. [4]. For example, for a solution containing 1.49 mM DEF and 8.00 mM $Na^+$ a peak potential shift (compared to a solution in the absence of $Li^+$) of 14 mV is observed. Of this, using the measured $k_{obs}$ value of $5.8 \times 10^3$ $M^{-1}$ $sec^{-1}$, 11 mV can be attributed to the following dimerization reaction. The residual 3 mV then yields an ion-pair formation constant $K$ of about 6 $M^{-1}$. This procedure gives $K$-values of 29, 6, and 2 for ion-pairs of $DEF^{\cdot-}$ with $Li^+$, $Na^+$, and $K^+$, respectively. These values seem to be generally in line with previously determined values of association constants in DMF; for example Peover and Davies (12) report a K of about 39 $M^{-1}$ for p-benzoquinone anion and $Li^+$ while Lasia and Kalinowski (15) report K's of 120 and 41 for ion pairs of $Li^+$ with fluorenone and indantrione radical anions, respectively. Using these $K$-values, a somewhat more detailed analysis of the kinetic data can be made. From the over-all rate expression for the reaction, Eq. [20], we find a $k_{obs}$ given by Eq. [22]

$$k_{obs} = (k_2 + k_{21}K[M^+] + k_{22}K^2[M^+]^2/(1 + K[M^+]^2) \quad [22]$$

Taking $K[M^+] = x$, this expression can be rearranged to

$$k_{obs}(1 + x)^2 - k_2 = k_{21}x + k_{22}x^2 \quad [23]$$

A plot of the left-hand side of [23] against $x$ allows

Table VIII. Rate constant for the dimerization of DBF and DEF radical anions in the presence of alkali metal ions[a]

| Olefin conc (m$M$) | Alkali metal ion conc [$M^+$], (mM) | $T_{Q.4}$ (msec) | $k_{obs}$ (l/mole-sec) | $k_{obs}/[M^+]$ ($l^2/m^2$-sec) |
|---|---|---|---|---|
| Dibutyl fumarate—Lithium iodide | | | | |
| 1.69 | 1.00 | 500.0 | $0.893 \times 10^3$ | $0.89 \times 10^6$ |
| 1.69 | 2.02 | 210.0 | 2.13 | 1.05 |
| 1.69 | 4.08 | 97.0 | 4.60 | 1.12 |
| 1.69 | 7.99 | 46.0 | 9.71 | 1.21 |
| 3.40 | 7.99 | 25.0 | 8.89 | 1.11 |
| | | | | Avg = $1.08 \times 10^6$ |
| Dibutyl fumarate—Sodium iodide | | | | |
| 1.99 | 1.00 | 887.0 | $0.428 \times 10^3$ | $4.31 \times 10^5$ |
| 1.98 | 2.91 | 370.0 | 1.00 | 3.54 |
| 1.96 | 5.76 | 219.0 | 1.76 | 3.11 |
| 1.91 | 11.3 | 135.0 | 2.93 | 2.63 |
| 1.82 | 21.8 | 71.0 | 5.82 | 2.67 |
| 3.00 | 21.8 | 44.0 | 5.78 | 2.65 |
| | | | | Avg = $2.92 \times 10^5$ |
| Diethyl fumarate—Lithium iodide | | | | |
| 1.13 | 1.04 | 357.0 | $1.87 \times 10^3$ | $1.79 \times 10^6$ |
| 1.13 | 2.00 | 167.0 | 4.00 | 2.00 |
| 1.13 | 3.04 | 108.0 | 6.19 | 2.03 |
| 1.13 | 4.41 | 73.0 | 9.15 | 2.07 |
| 2.01 | 4.41 | 42.0 | 8.94 | 2.03 |
| 2.01 | 6.72 | 26.0 | 14.4 | 2.14 |
| 2.01 | 8.90 | 18.0 | 20.8 | 2.33 |
| | | | | Avg = $2.05 \times 10^6$ |
| Diethyl fumarate—Sodium iodide | | | | |
| 1.49 | 1.00 | 920.0 | $0.551 \times 10^3$ | $5.51 \times 10^5$ |
| 1.49 | 2.00 | 400.0 | 1.27 | 6.33 |
| 1.49 | 4.00 | 188.0 | 2.70 | 6.73 |
| 1.49 | 8.00 | 88.0 | 5.76 | 7.19 |
| 2.94 | 8.00 | 52.0 | 5.14 | 6.42 |
| | | | | Avg = $6.43 \times 10^5$ |
| Diethyl fumarate—Potassium iodide | | | | |
| 3.42 | 1.13 | 1850.0 | 119 | $10.5 \times 10^4$ |
| 3.41 | 2.25 | 1260.0 | 176 | 7.78 |
| 3.40 | 3.36 | 855.0 | 260 | 7.74 |
| 3.36 | 5.56 | 513.0 | 438 | 7.88 |
| 3.32 | 8.77 | 365.0 | 623 | 7.10 |
| 3.31 | 12.9 | 266.0 | 858 | 6.64 |
| 6.02 | 12.9 | 149.0 | 840 | 6.50 |
| | | | | Avg = $7.27 \times 10^4$ |

[a] All solutions contained 0.2$M$ TBAI in DMF.

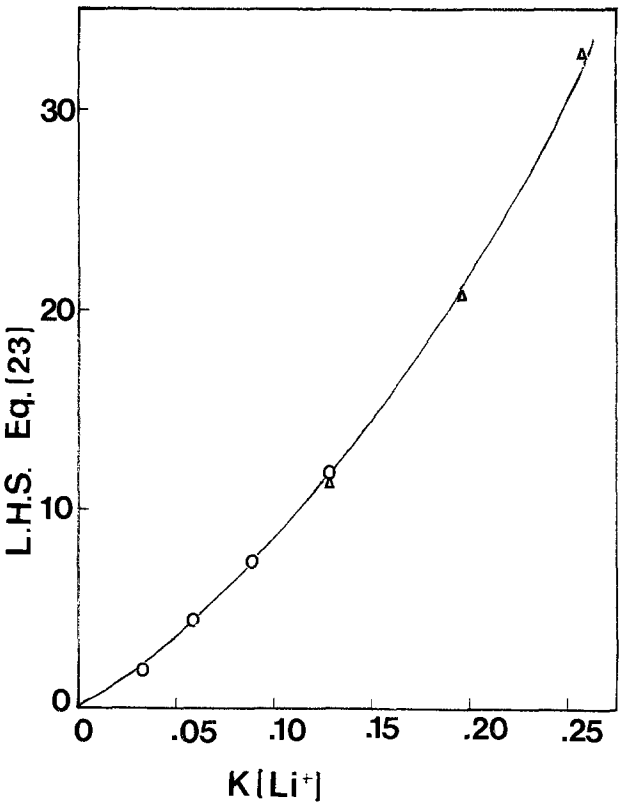


**Fig. 8. Variation of lefthand side of Eq. [23] (equal to $k_{obs}(1 + K[Li^+])^2 - k_2$) against $K[Li^+]$ with the data for the electroreduction of diethyl fumarate in 0.20M TBAI-DMF. The points are the experimental results at (○) 1.13 mM DEF and (△) 2.01 mM DEF and the line the calculated result with the rate constants listed in Table IX.**

one to estimate the $k_{21}$ and $k_{22}$-values; a typical plot for DEF-LiI is shown in Fig. 8. The values of $k_{21}$ and $k_{22}$ estimated by this procedure are given in Table IX. (A similar calculation for DBF, assuming the $K$-values for $DBF^{\cdot-}$ are the same as $DEF^{\cdot-}$ yields $3.2 \times 10^4$ and $5.7 \times 10^4$ $M^{-1}$ $sec^{-1}$ for $k_{21}$ with LiI and NaI, respectively). Extension of rate measurements to higher $M^+$ concentrations to obtain more reliable values for $k_{22}$ were limited by the reaction becoming too fast to measure by our techniques for $Li^+$, and the appearance of electrode filming in the case of $Na^+$ and $K^+$.

We have assumed in this treatment negligible association of the metal ions with supporting electrolyte ($I^-$) ion. This appears to be in agreement with previous measurements on alkali metal ion iodides and perchlorates in DMF (12, 32). Several experiments were also performed using $LiNO_3$ or $KNO_3$ (instead of the iodides) in the 0.2M TBAI-DMF solvent on the electroreduction of DEF. While the second-order dependence in DEF and primarily first-order dependence in metal ion was still observed, the $k_{obs}/[M^+]$ values obtained ($6.6 \times 10^6$ and $1.1 \times 10^6$ $M^{-1}$ $sec^{-1}$ for $LiNO_3$ and $NaNO_3$, respectively) were about twice those of the iodide salts. The reasons for these differences, which are well outside the experimental error limits of the measurements, are not clear, but suggest that impurities (e.g., water of hydration), adventitiously added with alkali metal ion salt, may have an effect on the reaction rate.

**Table IX. Summary of rate constants for dimerization of diethyl fumarate in presence of alkali metal ions[a]**

| System | $K$ ($M^{-1}$) | $k_2$ | $k_{21}$ ($M^{-1}$ $sec^{-1}$) | $k_{22}$ | $k_2K$[b] |
|---|---|---|---|---|---|
| DEF-LiI | 29 | 44 | $6.2 \times 10^4$ | $2.4 \times 10^5$ | $1.8 \times 10^6$ |
| DEF-NaI | 6 | 44 | $9.3 \times 10^4$ | $9 \times 10^5$ | $5.6 \times 10^5$ |
| DEF-KI | 2 | 44 | $3.3 \times 10^4$ | — | $1.3 \times 10^5$ |

[a] In 0.1M TBAI-DMF.
[b] Compare to Table VIII, $k_{obs}/[M^+]$.

## Discussion

The results generally show that reductive coupling of 1,2-diactivated olefins involve dimerization of radical anions both in the absence and presence of alkali metal ions. Adsorption of the parent olefins or the radical ions does not appear to be an important step in the reaction sequence. The linearity of the $Q - t^{1/2}$ plots suggests that the polymerization reactions which are of importance on the controlled potential coulometric time scale, do not interfere with the short time voltammetric measurements. In agreement with the previous results (2) we have found that addition of $Li^+$ decreases the extent of polymerization on bulk electrolysis. The mode by which this occurs has not been established, however two possibilities appear reasonable. If the dimer dianion, $R_2^{2-}$, is ion-paired with $Li^+$, it may be less reactive towards $R$ and so show less polymerization. If this were the case, however, it is difficult to understand why $Na^+$ and $K^+$ have such a small effect on the coulometric results. A second possibility is that $Li^+$ increases the rate of protonation of $R_2^{2-}$. $Li^+$ is known to be quite acidic and hence coordinates strongly with traces of water in the DMF. This coordinated water will be a better proton donor than uncoordinated water and may be brought to close proximity to the dimer dianion by the ion-paired $Li^+$. $Na^+$ and $K^+$ should show this effect to a much more limited extent. The increased acidity of water in the presence of $Li^+$ apparently does not cause appreciable protonation of the radical anion itself, since no evidence of the 2e reduction products was found. Additional evidence of the higher proton availability in the presence of $Li^+$ are the small bubbles observed during coulometry when $Li^+$ is present. These probably are caused by a small amount of $H^+$-reduction at the electrode, concurrent with olefin reduction, forming some hydrogen gas bubbles. Electrode filming in the presence of the alkali metal ions, especially at higher concentrations can be attributed to the formation of insoluble hydroxides upon hydrolysis (*i.e.*, deprotonation) of the aquated ions. Similar hydrolysis of metal ions and filming have been observed in nonaqueous solvents (33, 34).

The study also provides some new information on the dependence of radical anion dimerization rate on structure. For the dialkyl fumarates, the dimerization rate constant and diffusion coefficients decrease in the order Me > Et > n-Bu. Apparently, the bulkier the alkyl group, the slower is the movement through solution and the more hindered the dimerization reaction. The rate of dimerization of ethyl cinnamate (EC) radical anions (140 $M^{-1}$ $sec^{-1}$), compared to that for DEF (44 $M^{-1}$ $sec^{-1}$) may at first appear anomalously large, since EC can be considered to have a structure between DEF (2 $-CO_2$ Et groups) and stilbene (2 phenyl groups), whose $R^{\cdot-}$ dimerization rate is very slow. However, consideration of the resonance structures of the radical anions of the two compounds suggests that while DEF has several structures where electron density is not on the ethylenic carbon, *e.g.*, structure

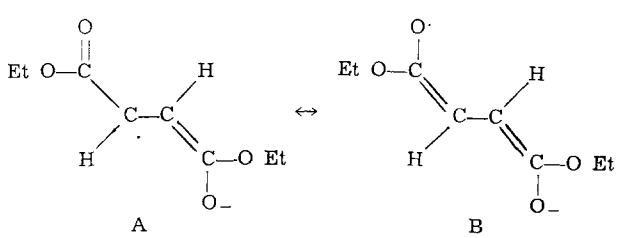


B, such structures are less probable for EC

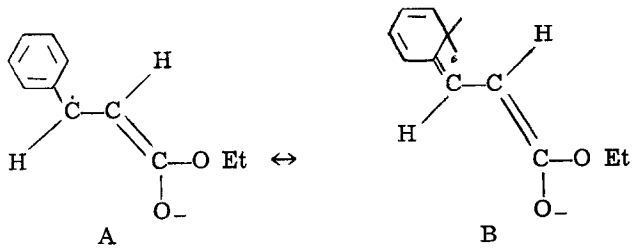


A B

Grypa and Maloy (35) recently also found a rate of disappearance of electrogenerated EC radical anion higher than that for DEF; their interpretation of the results differs from that given here, however.

The major conclusion of this study is that alkali metal ions increase the dimerization rate of radical anions by ion pair formation, thereby decreasing the electrostatic repulsion in the coupling of the bare anions. The reaction is predominantly first order in metal ion at low $Li^+$ and $Na^+$ and all $K^+$ concentrations, leading to a mechanism involving reaction of free radical anion with ion pair. At higher $Li^+$ and $Na^+$ concentrations coupling of two ion pairs becomes significant. Considering the results for DEF (Table IX) where fairly similar $k_{21}$-values are observed for the different alkali metal ions, we can speculate that the rate of the ion pair-radical anion reaction is roughly independent of metal ion and the different over-all rates observed depend upon different ion pair association constants. After this work was completed a note by Ryan and Evans (36) appeared in which the effect of $Na^+$ on DEF hydrodimerization in DMSO was investigated. Although the free anion dimerization rate in that solvent was much larger than that found in DMF, their values for $k_{21}$ and $k_{22}$ were remarkably close to those found in this study.

## Acknowledgment

The support of the Robert A. Welch Foundation and the National Science Foundation (GP-31414X) is gratefully acknowledged.

Manuscript submitted July 29, 1974; revised manuscript received Sept. 16, 1974.

Any discussion of this paper will appear in a Discussion Section to be published in the December 1975 JOURNAL. All discussions for the December 1975. Discussion Section should be submitted by Aug. 1, 1975.

*Publication costs of this article were partially assisted by The University of Texas at Austin.*

## REFERENCES

1. M. M. Baizer, in "Organic Electrochemistry," M. M. Baizer, Editor, Chap. XIX, Marcel Dekker, Inc., New York (1973).
2. W. V. Childs, J. T. Maloy, C. P. Keszthelyi, and A. J. Bard, *This Journal*, **118**, 874 (1971).
3. V. J. Puglisi and A. J. Bard, *ibid.*, **119**, 829 (1972).
4. V. J. Puglisi and A. J. Bard, *ibid.*, **120**, 748 (1973).
5. I. B. Goldberg, D. Boyd, R. Hirasawa, and A. J. Bard, *J. Phys. Chem.*, **78**, 295 (1974).
6. E. Lamy, L. Nadjo, and J. M. Savéant, *J. Electroanal. Chem.*, **42**, 189 (1973) and numerous references therein.
7. E. Lamy, L. Nadjo, and J. M. Savéant, *ibid.*, **50**, 141 (1974).
8. S. C. Rifkin and D. H. Evans, *This Journal*, **121**, 769 (1974) and references therein.
9. J. W. Hayes, I. Ruzić, D. E. Smith, A. L. Booman, and J. R. Delmastro, *J. Electroanal. Chem.*, **51**, 269 (1974).
10. J. P. Petrovich and M. M. Baizer, *This Journal*, **118**, 447 (1971).
11. M. Szwarc, "Carbanions, Living Polymers and Electron Transfer Processes," Interscience, New York (1968); *Accts. Chem. Res.*, **2**, 87 (1969).
12. L. Holleck and D. Becher, *J. Electroanal. Chem.*, **4**, 321 (1962); M. E. Peover and J. D. Davies, *ibid.*, **6**, 46 (1963).
13. T. Fujinaga, K. Izutsu, and T. Normura, *ibid.*, **29**, 203 (1971).
14. T. M. Krygowski, *ibid.*, **35**, 436 (1972); T. M. Krygowski, M. Lipsztajn, and Z. Galus, *ibid.*, **42**, 261 (1973); M. Lipsztajn, T. M. Krygowski, and Z. Galus, *ibid.*, **49**, 17 (1974).
15. M. K. Kalinowski, *Chem. Phys. Letters*, **7**, 55 (1970); *ibid.*, **8**, 378 (1971); A. Lasia and M. K. Kalinowski, *J. Electroanal. Chem.*, **30**, 511 (1972).
16. R. H. Philp, T. Layloff, and R. N. Adams, *This Journal*, **111**, 1189 (1964).
17. A. Lasia, *J. Electroanal. Chem.*, **42**, 253 (1973).
18. J. H. Christie, R. A. Osteryoung, and F. C. Anson, *ibid.*, **13**, 236 (1967).
19. F. C. Anson, *Anal. Chem.*, **38**, 54 (1966).
20. M. J. Hazelrigg and A. J. Bard, *J. Electroanal. Chem.*, **46**, 141 (1973).
21. M. J. Hazelrigg, Jr., Ph.D. Dissertation, The University of Texas at Austin, 1973.
22. F. C. Anson and D. A. Payne, *J. Electroanal. Chem.*, **13**, 35 (1967).
23. D. A. Payne, Ph. D. Dissertation, The University of Texas at Austin, 1970.
24. D. A. Payne and A. J. Bard, *This Journal*, **119**, 1665 (1972).
25. E. R. Brown, D. E. Smith, and G. L. Booman, *Anal. Chem.*, **40**, 1141 (1968).
26. G. Lauer and R. A. Osteryoung, *ibid.*, **40**, 30A (1968).
27. G. Lauer, R. Abel, and F. C. Anson, *ibid.*, **39**, 765 (1967).
28. R. A. Osteryoung, in "Electrochemistry," J. S. Mattson *et al.*, Editors, Chap. 11, Marcel Dekker, Inc., New York (1972).
29. S. P. Perone, in "Electrochemistry," J. S. Mattson *et al.*, Editors, Chap. 13, Marcel Dekker, Inc., New York (1972).
30. S. W. Feldberg, "Electroanalytical Chemistry," A. J. Bard, Editor, Vol. 3, Marcel Dekker, Inc., New York (1969).
31. M. L. Olmstead, R. G. Hamilton, and R. S. Nicholson, *Anal. Chem.*, **41**, 260 (1969).
32. (a) D. P. Ames and P. G. Sears, *J. Phys. Chem.*, **59**, 16 (1955). (b) P. G. Sears, E. D. Wilholt, and L. R. Dawson, *ibid.*, **59**, 373 (1955).
33. I. M. Kolthoff and J. F. Coetzee, *J. Am. Chem. Soc.*, **79**, 1852 (1957).
34. B. F. Myasoedov, I. S. Sklyarenko, and Yu. M. Kulyako, *Russian J. Inorganic Chem.*, **17**, 1541 (1972).
35. R. D. Grypa and J. T. Maloy, Private communication.
36. M. D. Ryan and D. H. Evans, *This Journal*, **121**, 881 (1974).